International Journal of Nanomedicine

Dovepress
Taylor & Francis Group

Open Access Full Text Article

ORIGINAL RESEARCH

Hypericin Nanoparticles-Associated Photodynamic Therapy Modulates the Biological Behavior of Hepatocellular Carcinoma by SERPINE1

Xuanzhi Yan[1,*], Jiaxing Fan[1,*], Wanying Qin[1,*], Minjun Liao[1,2,*], Siming Li[1], Liya Suo[1], Yujin Xie[1], Xin Jiang[3], Dengfeng Zou[4], Weijia Liao[1]

[1]Laboratory of Hepatobiliary and Pancreatic Surgery, Affiliated Hospital of Guilin Medical University, Guilin, Guangxi, 541001, People's Republic of China; [2]Peking University People's Hospital, Peking University Hepatology Institute, Beijing Key Laboratory of Hepatitis C and Immunotherapy for Liver Disease, Beijing, 100044, People's Republic of China; [3]Guangxi Key Laboratory of Drug Discovery and Optimization, Affiliated Hospital of Guilin Medical University, Guilin, Guangxi, 541001, People's Republic of China; [4]Guangxi Key Laboratory of Drug Discovery and Optimization, School of Pharmacy, Guilin Medical University, Guilin, Guangxi, 541199, People's Republic of China

*These authors contributed equally to this work

Correspondence: Weijia Liao, Laboratory of Hepatobiliary and Pancreatic Surgery, Affiliated Hospital of Guilin Medical University, Guilin, Guangxi, 541001, People's Republic of China, Email liaoweijia288@163.com; Dengfeng Zou, Guangxi Key Laboratory of Drug Discovery and Optimization, School of Pharmacy, Guilin Medical University, Guilin, Guangxi, 541199, People's Republic of China, Email zdf1226@163.com

Background: In recent years, photodynamic therapy (PDT) has gradually attracted the attention of researchers due to its therapeutic potential for treating malignant tumors. Hypericin (HC) is anticipated to enhance the therapeutic effect on tumors as an efficient photosensitizer (PS) for PDT. However, the role and mechanism of PDT in hepatocellular carcinoma (HCC) remain unclear.

Methods: In this study, we investigated the efficacy of hypericin nanoparticles (HC-NPs)-associated PDT (HC-NPs-PDT) on HCC to explore its anti-HCC mechanism both in vitro and in vivo. Cellular molecular experiments, as well as HCC mouse tumor models, were utilized to validate the impact of HC-NPs-PDT on HCC. Additionally, molecular docking and related experiments were employed to investigate its potential mechanism.

Results: Our findings demonstrated that HC-NPs-PDT effectively inhibits the viability, migration, and invasion abilities of HCC cells, as well as suppresses the growth of subcutaneous HCC tumors in BALB/C-nu nude mice. SERPINE1 (also known as PAI, PAI-1, PAI1, PLANH1) may be a key target of HC, as its mRNA and protein levels were significantly up-regulated following HC-NPs-PDT. This upregulation led to a decrease in mitochondrial membrane potential and promoted apoptosis of HCC cells. Additionally, inhibition of SERPINE1 partially restored changes in mitochondrial membrane potential.

Conclusion: These results suggest that HC-NPs-PDT may regulate the biological behavior of HCC by upregulating SERPINE1 expression, offering a new perspective for treating HCC.

Keywords: hepatocellular carcinoma, photodynamic therapy, hypericin, SERPINE1, biological behavior

Introduction

Liver cancer is the sixth most common malignant tumor worldwide, with an overall poor prognosis, and has become the third most lethal cancer worldwide.[1] Several studies have indicated that the incidence of hepatocellular Carcinoma (HCC), the most common type of liver cancer, continues to rise worldwide, and it is projected that more than 1 million people will be affected by HCC by 2025,[2] which represents a significant burden on human health and social development and requires urgent attention. Currently, the clinical treatments for HCC mainly include surgical treatment, ablation, liver transplantation, and comprehensive treatment.[3] The therapeutic effect of HCC is influenced by numerous factors,[4] and most HCC patients were diagnosed at an advanced stage, potentially missing the opportunity for radical treatment.[5,6] Consequently, the overall therapeutic efficacy of

Received: 29 November 2024
Accepted: 12 March 2025
Published: 20 March 2025

Graphical Abstract

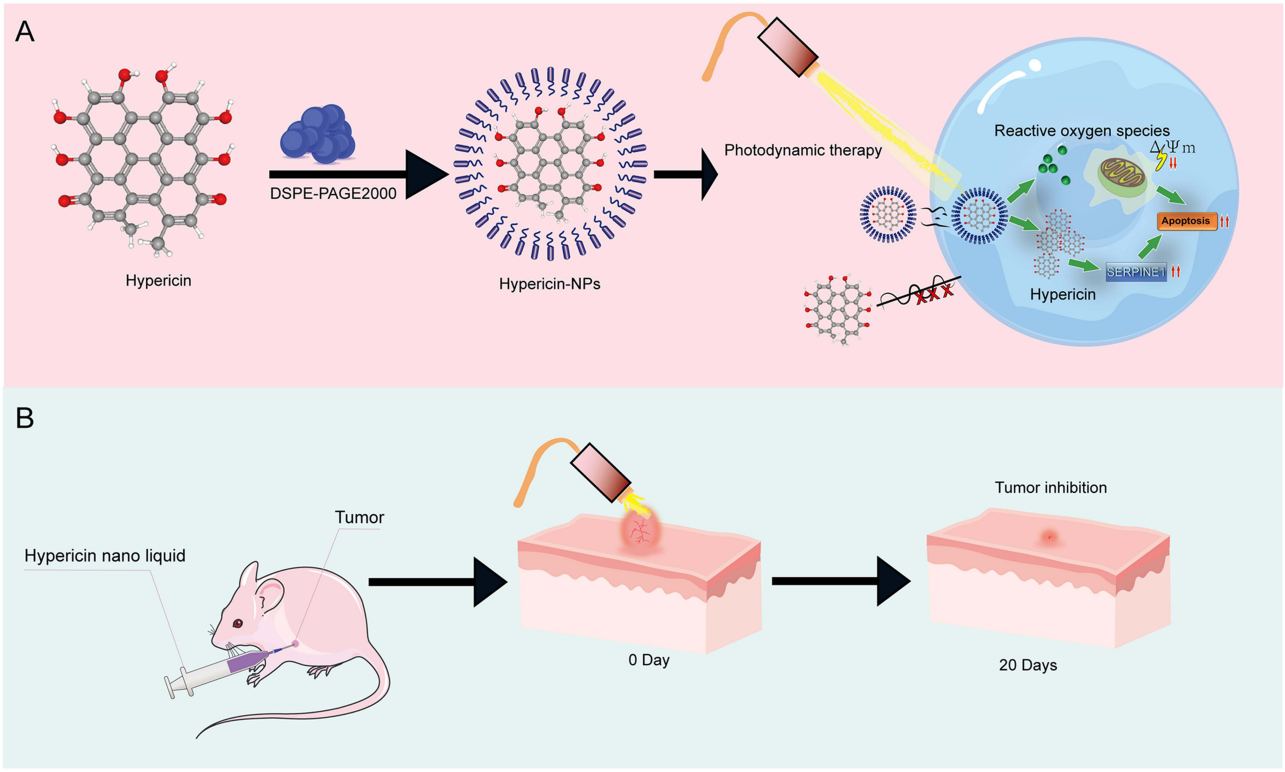

HCC is not favorable. Although current immunotherapy and targeted therapies have brought new hope to patients with HCC, only a small proportion of the patient population benefited from therapy in terms of overall survival (OS), with the possibility of drug resistance and adverse events during treatment also being present.[7,8] Therefore, more effective treatment strategies are needed.

Photodynamic therapy (PDT) is a diagnostic and therapeutic method that utilizes three key elements: photosensitizer (PS), light, and reactive oxygen species (ROS). The fundamental principle of PDT involves the absorption of excitation light of a specific wavelength by the PS. This then undergoes a photochemical reaction with surrounding oxygen, generating cytotoxic ROS capable of damaging and killing tumor cells. The generation of ROS is crucial for effectively eradicating tumor cells.[9] Recent studies have suggested that PDT may present a promising approach for treating nasopharyngeal carcinoma, lung cancer, bladder cancer, colon cancer, and other cancers.[10–12] Hypericin (HC) is a natural polycyclic aromatic naphthalene dibenzyl anthracene clover anthracene primarily found in hypericum species. It serves as a significant secondary product in most hypericum species. Previous research has indicated that HC exhibits diverse pharmacological activities including antitumor, antibacterial, antiviral, and neuroprotective effects.[13–15] Furthermore, HC shows considerable potential in PDT.[16] Pharmacokinetic assays have suggested inadequate water solubility and bioavailability of HC. Studies have demonstrated that nanoencapsulation of parthenolide significantly enhances therapeutic efficacy and improves physicochemical properties compared to unencapsulated drugs.[17] Utilizing nanoencapsulation technology not only enhances drug effectiveness but also improves target activity while reducing drug toxicity and side effects.[18,19]

This study aims to assess the impact of HC-NPs-PDT on the biological behaviors of HCC cells and explore potential mechanisms through in vivo and in vitro experiments. The findings will offer further support for clinical HCC treatment.

Materials and Methods

Materials

The principal materials and reagents were procured from the following sources. Hypericin (CAS No: 548–04-9) was obtained from Chengdu DeSiTe Biological Technology Co., Ltd (Sichuan, China). 1.2-distearoyl-sn-glycero-3-phosphoethanolamine-N-[methoxy(polyethyleneglycol)2000] (DSPE-PEG2000) (Cat No: PS1-E1-2K) was acquired from Ponsure (Shanghai, China). Fetal bovine serum (FBS) and Dulbecco's Modified Eagle's medium (DMEM) were obtained from NCM Biotech (Jiangsu, China). Reactive oxygen species assay kit (DCFH-DA) and the mitochondrial membrane potential assay kit (JC-1) were provided by Beyotime (Shanghai, China). Transwell migration chambers and invasion chambers were sourced from CORNING (USA). The Annexin V/PI apoptosis assay kit was bought from BD Biosciences (USA). Cell counting kit-8 (CCK-8) assay Kit was provided by DOJINDO (Shanghai, China). Anti-SERPINE1 antibody (Cat No: 13801-1-AP), anti-β-ACTIN antibody (Cat No: 66009-1-Ig) and anti-BCL-2 antibody (Cat No: 12789-1-AP) were obtained from ProteinTech (Hubei, China); anti-P53 antibody (Cat No: 4667S), anti-p-P53 antibody (Cat No: 9286S), anti-AKT antibody (Cat No: 4685S), anti-p-AKT antibody (Cat No: 12694S) were bought from Cell Signaling Technology (USA); anti-BAX antibody (Cat No: A18642) and anti-CASPASE3 antibody (Cat No: A19654) were provided by ABclonal (Wuhan, China). Additionally, the remaining reagents not previously mentioned can be readily obtained from commercial sources.

Methods

The Preparation and Characterization of HC-NPs

DSPE-PEG2000 is considered an ideal packaging material for nano-formulations due to its amphiphilic nature, excellent biocompatibility, and biodegradability. The HC-NPs were prepared using the nanoprecipitation method. The final HC-NPs solution was stored at 4°C, protected from light. The particle size of HC-NPs was assessed using electron microscopy. For specific configuration methods and comprehensive characterization of the material, tests have been performed by our collaborators and published in an article.[20].

Cell Culture

The Bel-7402 and Huh7 cell lines were generously provided by Prof. Hongsong Chen (Institute of Liver Diseases, Peking University). The cells were cultured in DMEM complete medium (containing 10% FBS, 1% penicillin-streptomycin double antibody) at 37 °C in a 5% CO_2 incubator.

Cytotoxicity Assay in vitro

The cytotoxicity of HC-NPs was assessed using a CCK-8 kit. Bel-7402 and Huh7 cells were seeded in 96-well plates at a density of 8×10^3 cells/well with 100 μL DMEM/well (with four replicates in each group). The cells were then incubated at 37 °C in a 5% CO_2 incubator for 24 h. After that, the medium was replaced with new medium containing different concentrations of HC-NPs. Following a 24-hour incubation period, the cells were exposed to light for varying periods of time (100 mW/cm²) using a xenon lamp (NO: CEL-S500, purchased from Beijing China Education Au-light Technology Co., Ltd). Subsequently, the complete medium was replaced with HC-NPs-free DMEM, and the cells were further incubated for another 24 h. Then, the complete medium containing CCK-8 working solution was added and incubated for 2 h in a light-avoiding environment. Finally, the absorbance at 450 nm was measured using a continuous-wavelength zymography instrument (Molecular Devices, USA) to calculate cell viability.

To enable a more comprehensive comparison of the effects of HC-NPs and HC aqueous solution, the experimental groups were defined as follows: the HC aqueous solution group, the HC aqueous solution combined with PDT group, the HC-NPs group, and the HC-NPs combined with PDT group. A range of drug concentration gradients were established in the seed plates, and the methodology and assays were carried out following previously described procedures.

Growth Curve Assay in vitro

To assess the long-term impact of HC-NPs-PDT on the viability of two HCC cell lines, a growth curve assay was conducted at designated time points. The experimental groups were as follows: control group, irradiation only group, HC-NPs only group, and HC-NPs with irradiation group. Bel-7402 and Huh7 cells were inoculated at a density of 3×10^5 cells/well in 6-well plates, with 2 mL DMEM/well. After the cells were irradiated with light (100 mW/cm^2, 10 min), all samples were replaced with fresh medium, and culture was continued for 24 h. Cells from each group were digested, resuspended, and inoculated in 96-well plates at a density of 8×10^3cells/well, 100 μL DMEM/well. Cell proliferation for each group was assessed at 6 h, 24 h, 48 h, 72 h, 96 h, and 120 h using the previously described cell viability assay method.

Intracellular ROS Quantification

The experimental groups were defined as follows: positive control group, blank control group, irradiation only group, HC-NPs only group, and HC-NPs with irradiation group. Bel-7402 and Huh7 cells were inoculated in 12-well plates at a density of 1×10^5 cells/well with 1 mL DMEM/well. After the administration of cells and subsequent illumination, the entire culture medium was replaced with fresh medium. Following a further 24-hour incubation period, 500 μL of Resoup (prepared at a 1:1000 dilution in serum-free medium) was added to the positive control group. The solution was then incubated at 37 °C for 20 minutes and subsequently washed three times with PBS. The reactive oxygen species probe (DCFH-DA) (prepared at a 1:1000 dilution in serum-free medium, 500 μL per group) was then added to all groups and incubated at 37 °C for a further 20 minutes. The samples were washed with PBS three times and photographed and imaged under a fluorescence microscope (Carl Zeiss AG, German).

Invasion and Migration Assay in vitro

The experimental groups were defined as follows: control group, irradiation only group, HC-NPs only group, and HC-NPs with irradiation group. After the administration of cells and subsequent illumination, the cells in each group were digested, resuspended, and inoculated into the upper compartment of Transwell (without matrix gel) and Transwell (with matrix gel) at a density of 3×10□ cells/well with 100 μL serum-free DMEM/well, respectively. A total of 600 μL of DMEM (containing 10% FBS) was added to the lower chamber. Following a 24-hour incubation period, the samples were fixed and stained. Subsequently, images were captured under an inverted phase-contrast microscope (Olympus, Japan).

Cell Cycle and Apoptosis Assay

The experimental groups were defined as follows: control group, irradiation only group, HC-NPs only group, and HC-NPs with irradiation group. After the administration of cells and subsequent illumination, cells from each group were collected and stained according to the instructions provided with the cell cycle and apoptosis assay kit. The stained cells were then analyzed using a flow cytometer (Agilent, USA).

Bioinformatics Analysis

A preliminary screening process was conducted based on the NCBI database, the String protein interaction network (https://cn.string-db.org/), and the Cytoscape algorithm. Subsequently, molecule-protein binding simulation was performed using drug molecule docking simulation software PYMOL. This process aimed to identify potential targets for HC.

qRT-PCR Assay

The experimental groups were defined as follows: control group, irradiation only group, HC-NPs only group, and HC-NPs with irradiation group. After the administration of cells and subsequent illumination, total RNA was extracted from each group using TRIZOL lysate. cDNA was then synthesized according to the instructions of the Reverse Transcription Kit (Takara, Japan). The PCR reaction system was configured according to the instructions of the TB Green® Premix Ex

TaqTM GC Kit (Takara, Japan), and amplification was carried out on a 7500 Quantitative PCR instrument (Thermo, USA). Primer sequences for this analysis are detailed in Table S1.

Mitochondrial Membrane Potential Assay in vitro

The mitochondrial membrane potential was quantified using a Mitochondrial membrane potential kit (JC-1). The experimental groups were defined as follows: control group, irradiation only group, HC-NPs only group, and HC-NPs with irradiation group. Following the administration of cells and subsequent illumination, CCCP (1:1000 dilution) was initially introduced to the positive control. It was then incubated at 37 °C for 20 minutes and washed three times with PBS. Subsequently, 1mL of the JC-1 working solution (1:160 dilution with JC-1 buffer) was added to each group. After incubating at 37 °C for 20 minutes, the samples were washed three times with JC-1 buffer. Finally, the samples were analyzed using a flow cytometer (Agilent, USA).

Western Blot (WB) Analysis

The expression of SERPINE1, P53, p-P53, AKT, p-AKT, BAX, BCL-2 and CASPASE3 following HC-NPs-PDT was determined through WB. The experimental groups were set as follows: control group, irradiation only group, HC-NPs only group, and HC-NPs with irradiation group. Following the administration of cells and subsequent illumination, total protein was extracted using RIPA lysate for each group. Total protein quantification was performed using a BCA kit. The visualization of protein expression involved a series of steps including electrophoresis, blocking, incubation with the primary antibody and secondary antibody, and finally detection through chemiluminescence on Tanon 5200 Series Fully Automated Chemiluminescent Image Analysis System.

Immunofluorescence (IF) Assay in vitro

The experimental groups were set as follows: control group, irradiation only group, HC-NPs only group, and HC-NPs with irradiation group. Following the administration of cells and subsequent illumination, the cells in each group were fixed, permeabilized, stained, incubated with primary antibody and secondary antibody and stained with DAPI to observe the expression of SERPINE1 under a fluorescence microscope (Carl Zeiss AG, German).

Evaluation of Antitumor Efficacy and Safety in vivo

All animals used in this study were treated in accordance with the *Guidance for the Care and Use of Laboratory Animals*. The study was conducted following ethical standards set forth by the Institutional Animal Care and Use Committee of Guilin Medical University (IACUC) and received ethical approval (ethical review number: GLMC-IACUC-20241055). The anti-tumor effect of HC-NPs-PDT was evaluated by establishing a Bel-7402 nude mouse subcutaneous xenograft tumor model. BALB/C-nu SPF-grade nude mice were purchased from Hunan Slaughter Kingda Laboratory Animal Co., Ltd. A total of 1×10□ Bel-7402 cells were injected subcutaneously into the right anterior dorsal region of the mice. Once the tumor volume reached 80–100 mm^3, the nude mice were randomly divided into four groups (control group, irradiation only group, HC-NPs only group, HC-NPs with irradiation group), with five mice in each group. Subsequent treatments (10 minutes of irradiation each) were performed every four days for a total of four photodynamic treatments. The anti-tumor effect was assessed by measuring the body weight and tumor volume of nude mice in each group every two days. The control and irradiation only groups were administered 120 μL of saline via intratumoral and peritumoral injections, while the HC-NPs only and HC-NPs with irradiation groups received 120 μL of HC-NPs solution (400 μg/kg). Following a two-hour period after drug injection, the irradiation only group and the HC-NPs with irradiation group were subjected to 10 minutes of light irradiation with a light intensity of 223 J/cm^2. The mice were euthanised after 20 days. Photographs were taken for record keeping, and tumor tissues collected for analysis using immunohistochemistry and other experiments to investigate molecular mechanisms related to drug action. The tumor volume was calculated according to the following Eq.: Volume = (Tumor Length) × $(\text{Tumor Width})^2/2$.

Immunohistochemistry (IHC) Assay

The subcutaneous tumors of nude mice were excised, fixed in 10% formalin, embedded in paraffin, deparaffinized and hydrated. Antigen retrieval was performed, followed by peroxidase inactivation and blocking of non-specific sites. The samples were then incubated with primary and secondary antibodies, developed, stained with hematoxylin, dehydrated, and sealed. Subsequently, they were photographed for observation under a microscope.

Statistics Analysis

The experimental data were analyzed using SPSS 20.0 statistical software. Normally distributed data, presented as mean ± standard deviation, were assessed using *t*-test and one-way ANOVA; non-normally distributed data were evaluated using non-parametric tests. A significance level of $p < 0.05$ was considered statistically significant (* $p < 0.05$, ** $p < 0.01$, *** $p < 0.001$, **** $p < 0.0001$). Graphs were created using GraphPad Prism 9.0 software.

Results

Preparation and Characterization of HC-NPs

HC-NPs were prepared by encapsulating HC (Figure 1A shows the structural formula) with DSPE-PEG2000, resulting in a thin coating film around the periphery of HC. The particles were well dispersed and had a size of < 200 nm (Figure 1B), meeting the standard for nanoparticles. This demonstrates the successful encapsulation of HC, as confirmed by transmission electron microscopy (TEM).

Optimal Conditions for HC-NPs-PDT

Cell viability assays were conducted using a range of HC-NPs concentrations (0, 40, 80, 120, 160, 200 ng/mL) and a variety of light durations (0, 5, 10, 15 min). It was observed that both HCC cell lines were affected by HC-NPs-PDT (Figure 2A and B), which showed a dose- and time-dependent effect. The optimal IC_{50} values of 120 ng/mL for Bel-7402 and 80 ng/mL for Huh7 were identified from the data analysis. Additionally, the optimal photodynamic time was determined to be 10 minutes. Previous studies on drugs have often focused on their pharmacological properties with less attention paid to their physical characteristics. However, in this study it was found that HC-NPs exhibited superior inhibitory effects on the viability of the two HCC cell lines under photodynamic conditions when compared to ordinary HC aqueous solvents (Figure 2C and D).

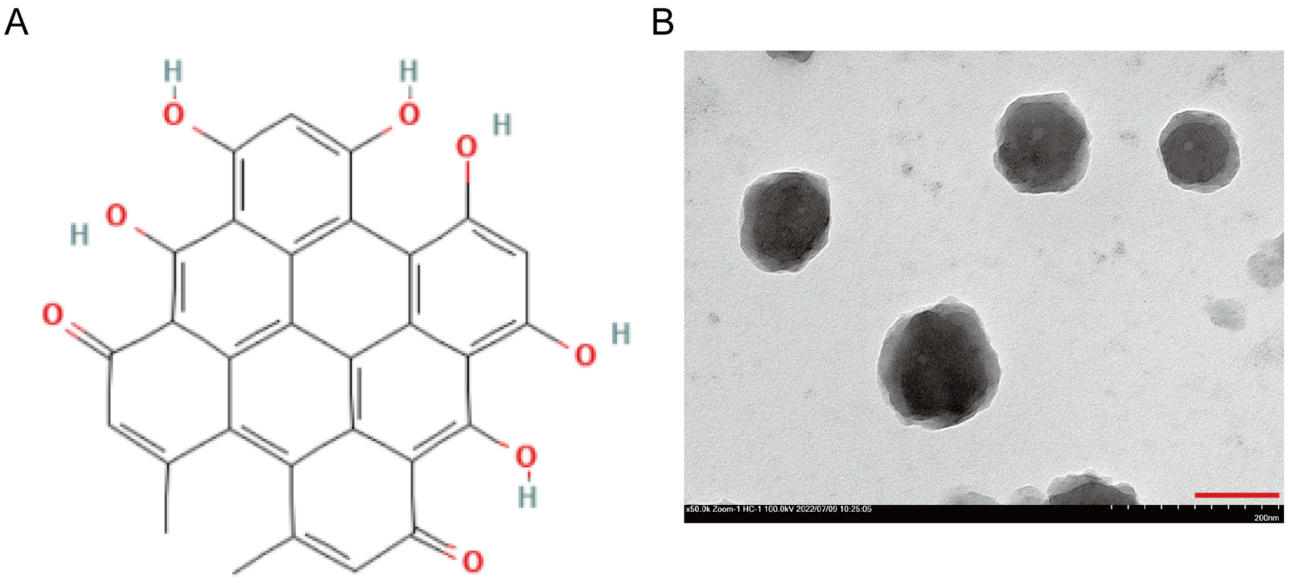

Figure 1 Diagram of the molecular structural formula of HC and electron micrograph of HC-NPs. (**A**) Molecular structural formula of HC; (**B**) Electron micrograph of HC-NPs (scale bar: 100 nm).

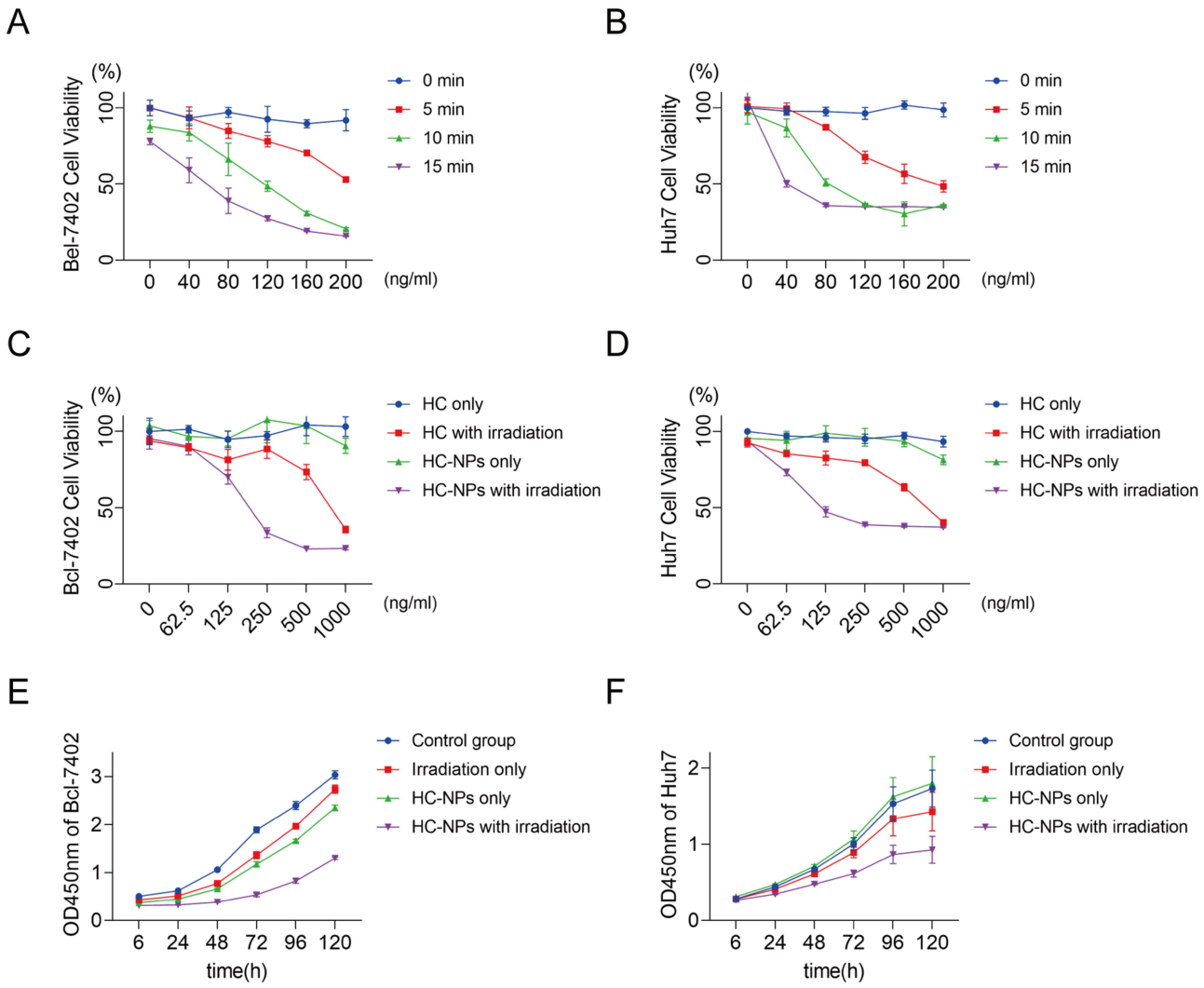

Figure 2 The photodynamic conditions of HC and comparing effects before and after HC nanocoating. (**A** and **B**) represent the effects of different concentrations of HC-NPs at different light times; (**C** and **D**) illustrate the effects of different concentrations of HC with or without nanocoating at the same light time; (**E** and **F**) represent the 120h growth curves of Bel-7402 and Huh7 under the same photodynamic conditions, respectively.

The impact of HC-NPs-PDT on the viability of the two HCC cell lines was assessed through growth curves. The results revealed that the long-term viability inhibition of HCC cells was significantly greater in the HC-NPs with irradiation group compared to the control group (Figure 2E and F).

Intracellular ROS Quantification

The primary mechanism of PDT involves the generation of ROS. In this study, we further investigated the efficiency of HC-NPs-PDT in generating ROS. As shown in Figure 3A–D, the levels of ROS in cells from different groups were assessed using the DCFH-DA probe, with untreated cells serving as a positive control. The results demonstrated that the group treated with HC-NPs with irradiation exhibited a significantly higher fluorescence signal for DCFH-DA compared to the other experimental groups, indicating that this treatment was capable of effectively generating a substantial quantity of ROS.

Migration and Invasion Assays

Based on the pre-established working conditions, we investigated the in vitro effects of HC-NPs on HCC cells. The results of the Transwell assay (without matrix gel) are presented in Figure 4A. The HC-NPs with irradiation group

https://doi.org/10.2147/IJN.S507037

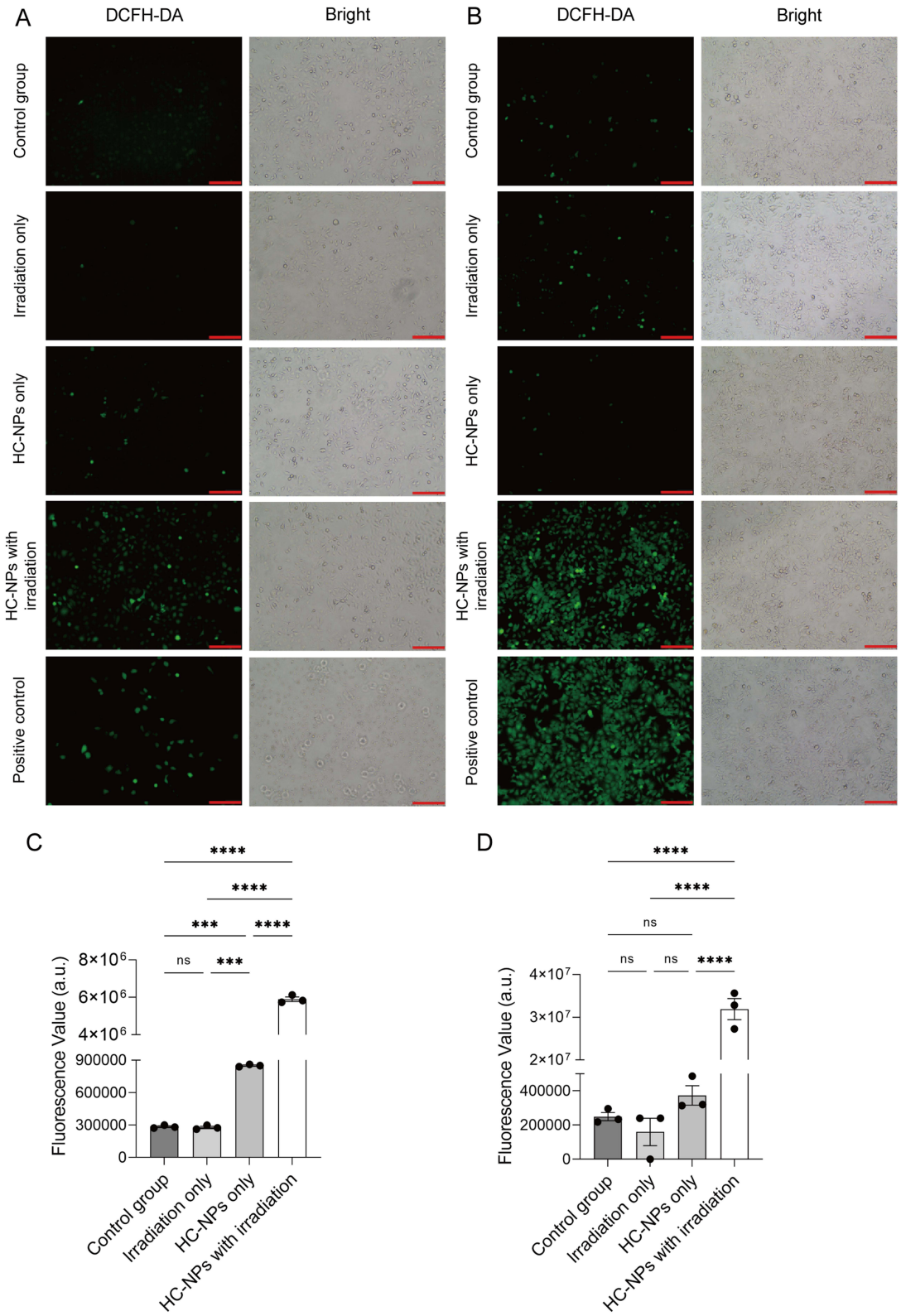

Figure 3 Detection of the output of reactive oxygen species from HC-NPs-PDT using DCFH-DA. (**A**–**C**) Fluorescence detection and statistical analysis of reactive oxygen species in Bel-7402; (**B**–**D**) Fluorescence detection and statistical analysis of reactive oxygen species in Huh7 (scar bar: 200 μm), (***p<0.001, ****p<0.0001).

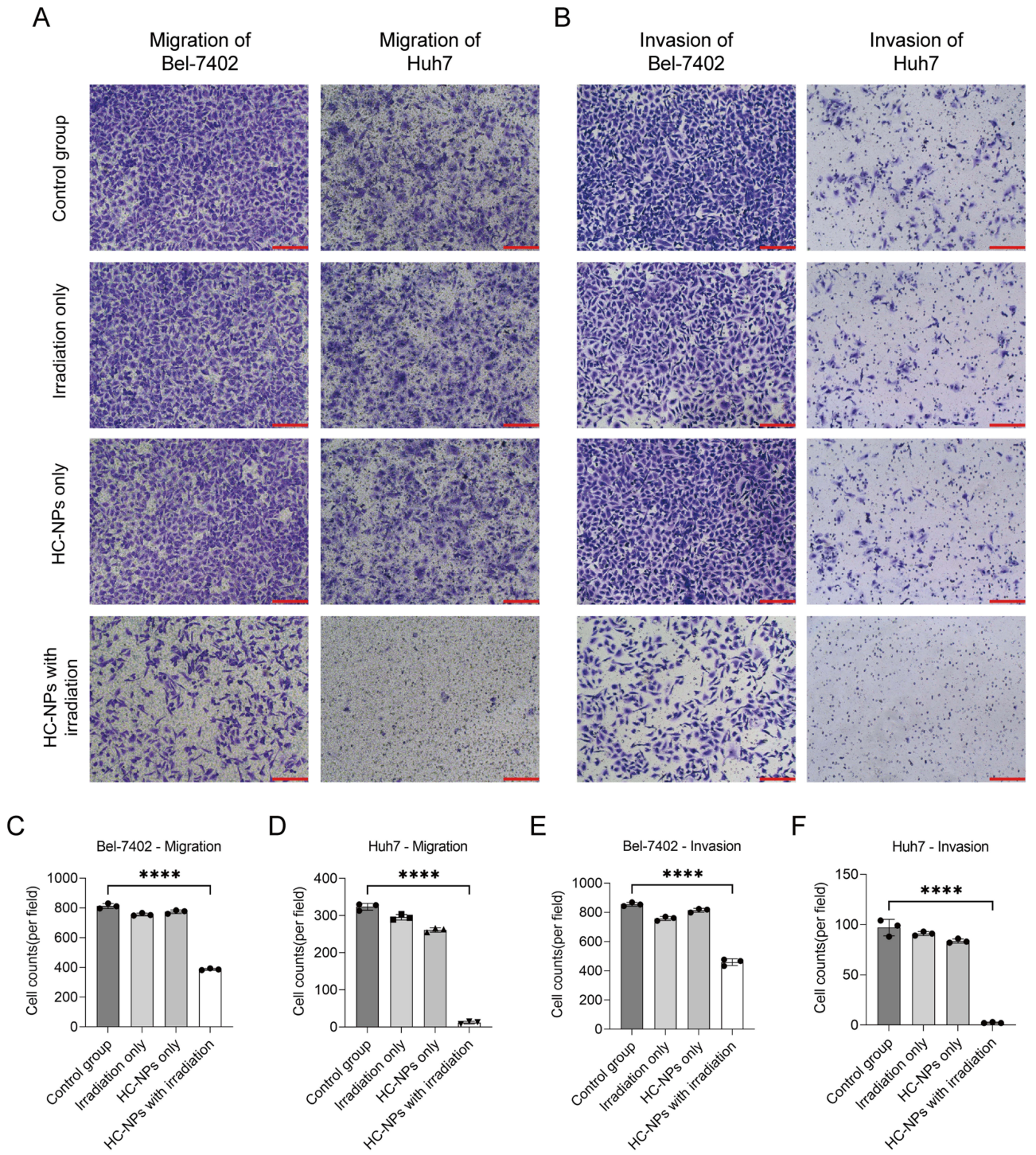

Figure 4 Transwell assay to detect the effect of HC-NPs-PDT on the migration and invasion ability of HCC cells. (**A** and **D**) Effects of HC-NPs-PDT on the migration ability of Bel-7402 and Huh7 cells and statistics; (**B** and **F**) Effects of HC-NPs-PDT on the invasion ability of Bel-7402 and Huh7 cells and statistics (scar bar: 200 μm), (****p<0.0001).

demonstrated a more pronounced inhibition of the migratory ability of HCC cell lines compared to the control group, the irradiation only group, and the HC-NPs only group. The Transwell assay (with matrix gel) is presented in Figure 4B. In comparison to the control group, the irradiation only group, and the HC-NPs only group, the HC-NPs with irradiation group showed a more pronounced inhibitory effect on the invasive capacity of HCC cell lines. Figure 4C–F present the statistical analysis of the results, respectively.

https://doi.org/10.2147/IJN.S507037

Effect of HC-NPs-PDT on Apoptosis and Cell Cycle Progression

The flow cytometry analysis (Figure 5A and B) revealed that the proportion of apoptotic cells (Q4-2 + Q4-4) was increased, while the normal state of HCC cells (Q4-3) was decreased in the HC-NPs with irradiation group compared to the control group, the irradiation only group, and the HC-NPs only group. These findings suggest that HC-NPs-PDT may induce apoptosis in HCC cells, with most apoptotic cells being in a late apoptotic state (Figure 5C and D). This observation was statistically significant ($p < 0.001$). Consequently, we examined alterations in relevant apoptotic products using WB. BAX and CASPASE3 protein levels were upregulated, while BCL-2 protein level was downregulated (Figure 5E) in Bel-7402 and Huh7 following administration of HC-NPs-PDT. We then investigated the effect of HC-NPs-PDT on the cell cycle of HCC cells by PI staining. The results showed (Figure S1B and D) that only the cell cycle of Huh7 cells was affected by HC-NPs-PDT, mainly interfering with the G2 phase, while Bel-7402 did not exhibit similar results (Figure S1A and C). After repeated experiments, we determined that HC-NPs-PDT had little effect on the cell cycle of HCC cells. Therefore, it can be inferred that HC-NPs-PDT can induce apoptosis in HCC cells further inhibiting their growth.

qRT-PCR Analysis

Based on the bioinformatics analysis, four candidate gene targets for HC were identified (Figure S2A). mRNA was then extracted from the control group, irradiation only group, HC-NPs only group, and HC-NPs with irradiation group of the two cell lines. The qRT-PCR analysis revealed that the mRNA level of SERPINE1 showed significant alterations in both Bel-7402 and Huh7 cells compared to the control group (Figure S2B and C). The other three genes exhibited less significant changes in mRNA levels, and their related results have not been presented. Therefore, SERPINE1 was identified as a key target for HC and subsequently selected for further experimental investigation.

Western Blot (WB) Analysis

Proteins were extracted from HCC cells in the control group, irradiation only group, HC-NPs only group, and HC-NPs with irradiation group. The WB results revealed up-regulated SERPINE1 expression in Bel-7402 and Huh7 cell lines of the HC-NPs with irradiation group (Figure 6A), which was consistent with the findings of the qRT-PCR analysis. Furthermore, we observed that the elevated expression of SERPINE1 was concomitant with the downregulation of P53/p-P53 and AKT/p-AKT (Figure 6A). And Figure 6B and C present the statistical results for 7402 and Huh7 cells, respectively. It was hypothesized that there was a correlation between the downregulation of P53/p-P53 and AKT/p-AKT and the upregulation of SERPINE1. In tumor cells, AKT and its phosphorylated form (p-AKT) are regarded as important molecules that regulate cell behaviors. The down-regulation of AKT/p-AKT protein expression could also verify that HC-NPs-PDT could regulate the biological behaviors of HCC cells, which is in agreement with the results of cytological experiments. Subsequently, the total proteins of Huh7 cells were extracted after 8 h, 24 h, and 48 h following HC-NPs-PDT. The protein expression of SERPINE1 gradually increased, while the protein expression of P53 and p-P53 gradually decreased with extension of treatment time. And the expression of SERPINE1 was negatively correlated with P53 (Figure S3). Consequently, it was postulated that the HC-NPs-PDT might have triggered SERPINE1 enhancement dependent of P53 protein depletion.

In conclusion, HC-NPs-PDT resulted in the upregulation of SERPINE1 protein expression in HCC cells.

Mitochondrial Membrane Potential Assay Analysis

Based on the combination of previous flow cytometry results and the subcellular localization of SEPRINE1, it's found that SERPINE1 is mainly concentrated in the cytoplasm and mitochondria of liver cancer cells after treatment (Figure S5A). We hypothesized that HC-NPs-PDT-induced apoptosis may be linked to the activation or inhibition of its targets, which are distributed in the cytoplasm and mitochondria. To investigate this further, we employed the JC-1 kit to detect mitochondrial membrane potential. The flow cytometry results (Figure 7) revealed a significant decrease in the E2 cell population and a notable increase in the E3 cell population following HC-NPs-PDT treatment ($p < 0.001$). These findings indicate that HC-

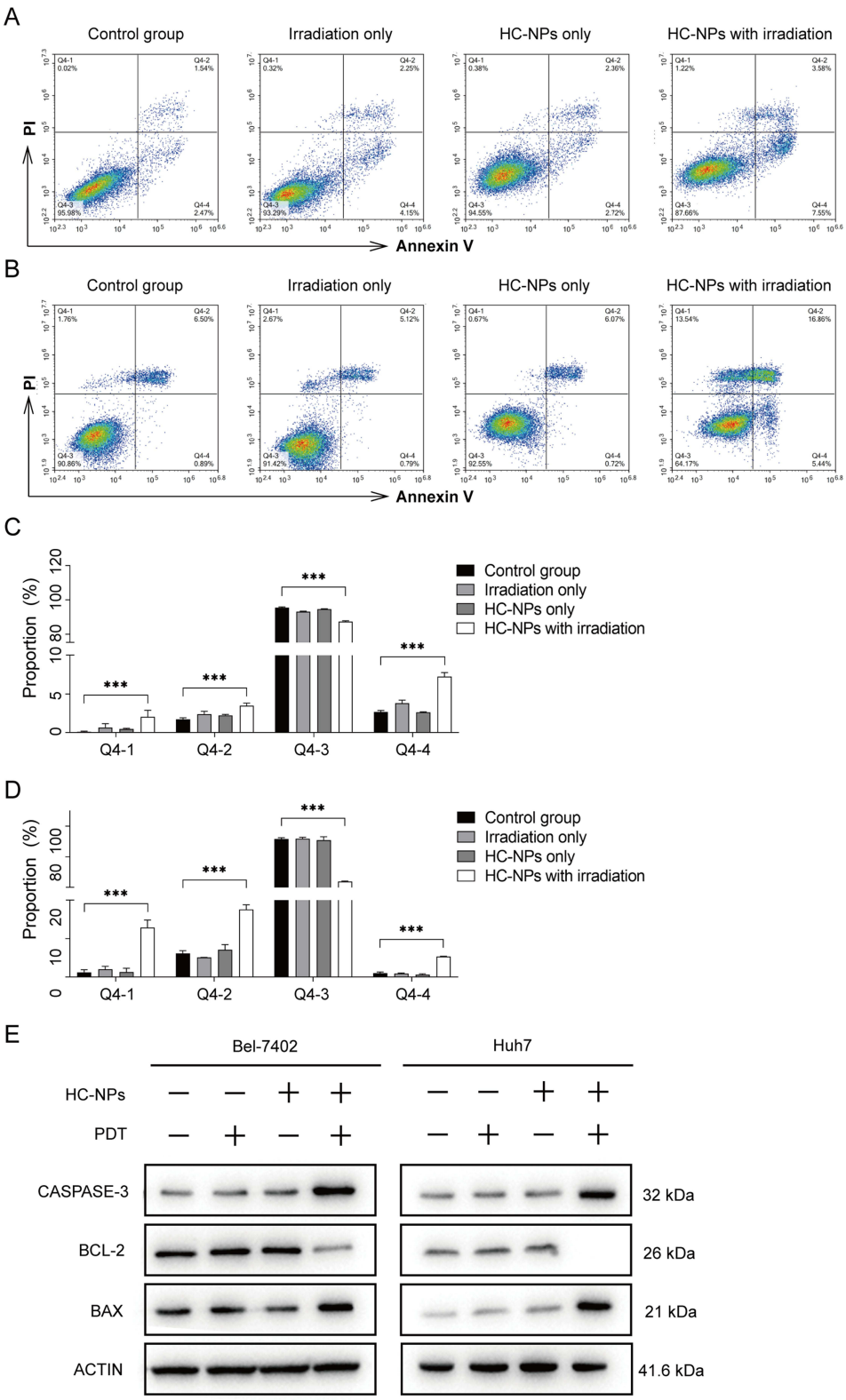

Figure 5 Utilization of Annexin V-FITC/PI staining for detection of apoptotic process using flow cytometry and data statistics. (**A**) Flow cytogram of Bel-7402-related apoptosis; (**B**) Flow cytogram of Huh7-related apoptosis; (**C** and **D**) represent the statistical analysis of the apoptotic process in Bel-7402 and Huh7, respectively, (***p<0.001); (**E**) shows the protein level related to apoptosis in Bel-7402 and Huh7.

https://doi.org/10.2147/IJN.S507037

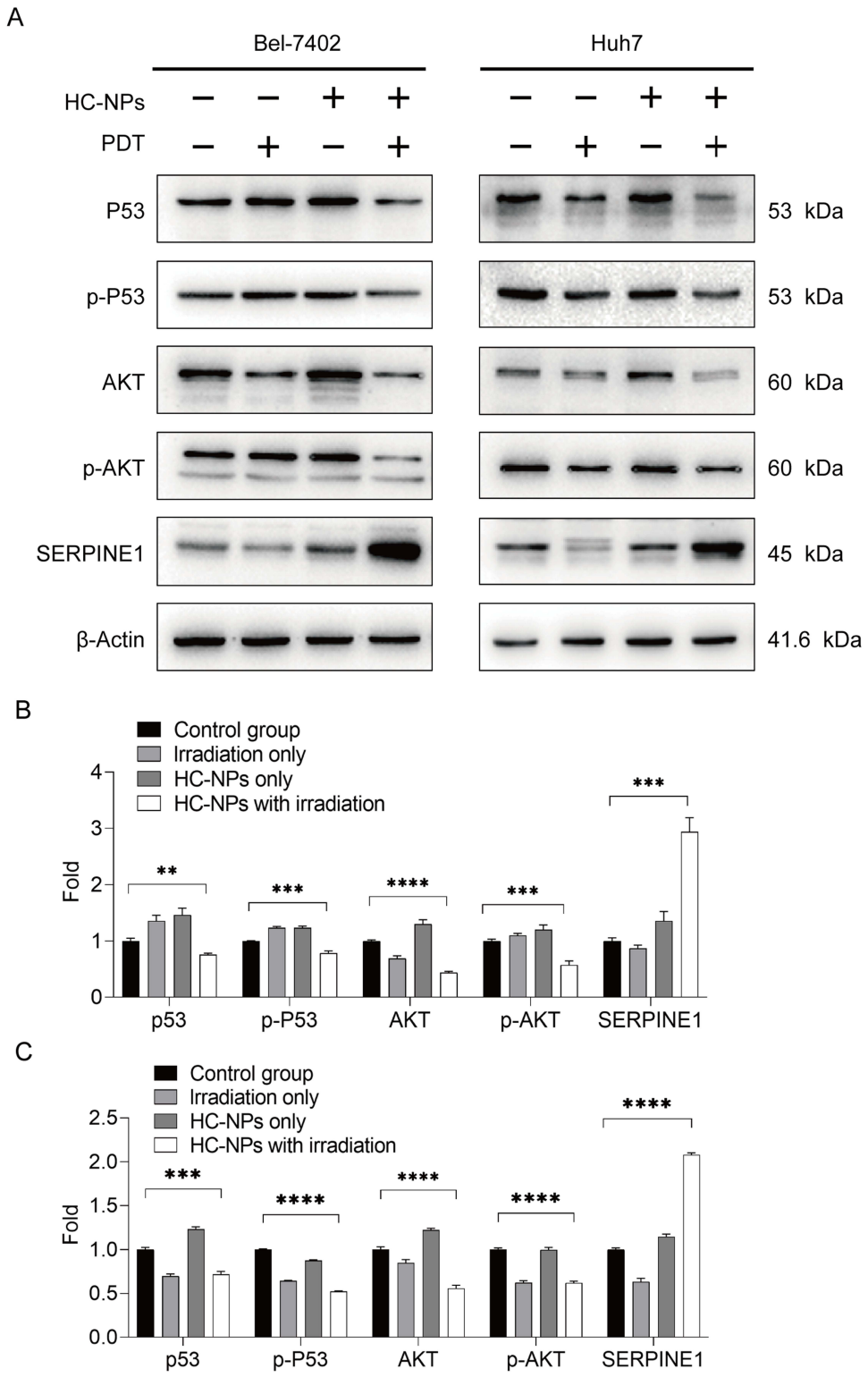

Figure 6 Graph of Western blot results. (**A**) displays the Western blot bands of different groups of Huh7 and Bel-7402; (**B**) presents the Western blot statistics of Bel-7402; (**C**) presents the Western blot statistics of Huh7, (***p*<0.01, ****p*<0.001, *****p*<0.0001).

NPs-PDT can reduce the mitochondrial membrane potential of Bel-7402 and Huh7 cells, leading to a substantial proportion of biologically normal cell populations becoming aberrant and ultimately inducing apoptosis.

Furthermore, in order to substantiate the regulatory role of SERPINE1 on HCC cells, we divided the two HCC cell lines into two groups: one with the addition of SERPINE1 inhibitor TM5275 (6 μg/mL) (MedChemExpress), and one

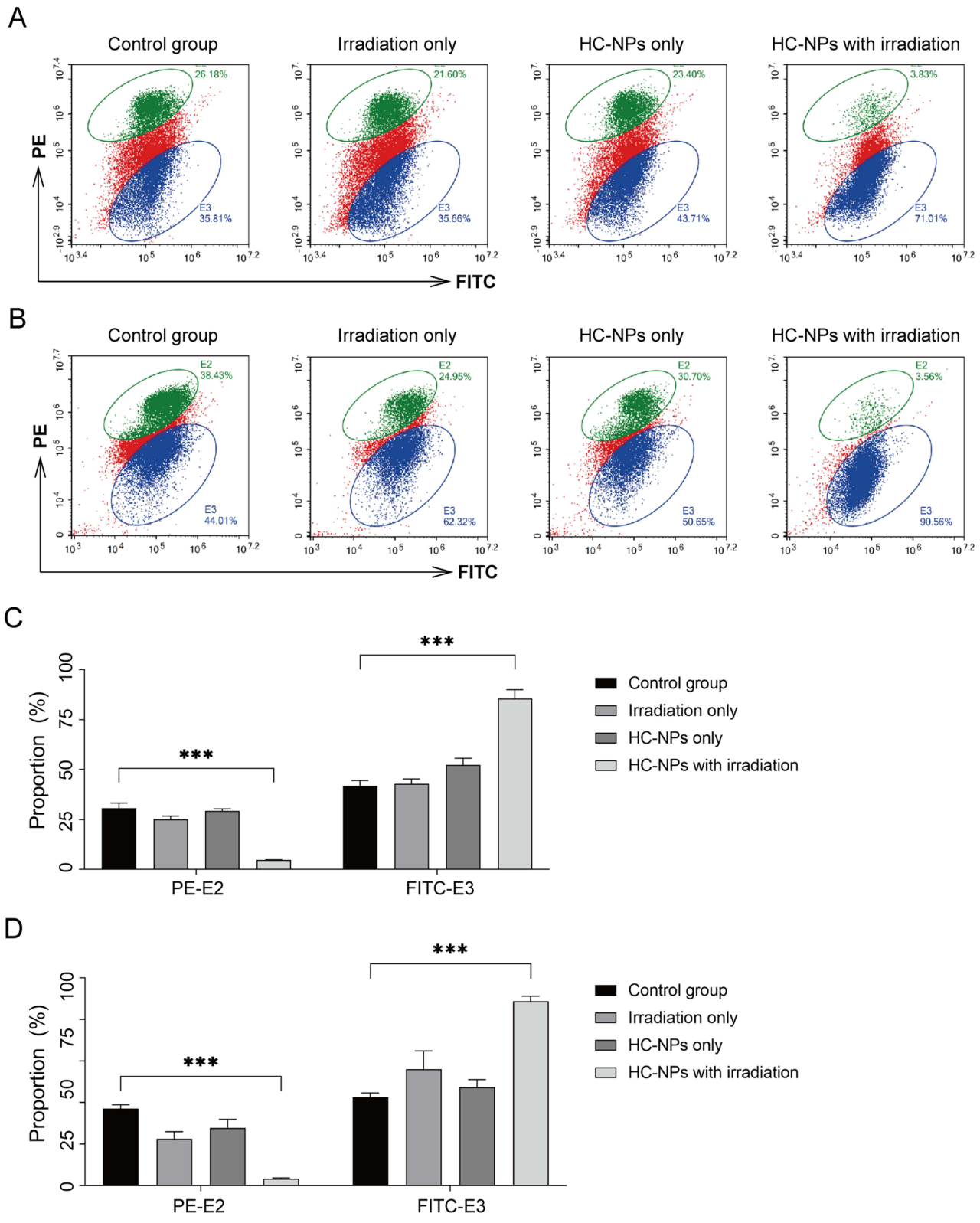

Figure 7 JC-1 kit to detect the effect of HC-NPs-PDT on mitochondria. (**A**–**C**) represent the JC-1 signals and corresponding statistical plots associated with Bel-7402 cells; (**B**–**D**) represent the JC-1 signals and statistical plots associated with Huh7 cells, (***p<0.001).

https://doi.org/10.2147/IJN.S507037

without it. A comparison of the results suggested that both cell lines in the HC-NPs with irradiation group (Figure S4A and B) exhibited consistency with previous findings, namely a decrease in membrane potential and a downward shift of the cell clumps. However, when the inhibitor TM5275 was added, there was an upward shift of some cell clumps and partial restoration of the membrane potential. This indicates that inhibiting SERPINE1 expression was beneficial for restoring mitochondrial membrane potential, reflecting SERPINE1's tumor suppression properties.

Photodynamic Therapy of Subcutaneous Tumors in vivo

In light of the impressive antitumor efficacy of HC-NPs-PDT observed in vitro, we established a human-derived xenograft tumor model to further evaluate its anticancer properties in vivo. The results revealed that the tumor growth was significantly slower and the total volume was markedly smaller in the HC-NPs with irradiation group compared to the control group, the irradiation only group and the HC-NPs only group ($p < 0.01$) (Figure 8). These findings suggest that HC-NPs-PDT can inhibit further growth of subcutaneous tumors.

Immunofluorescence (IF) and Immunohistochemical (IHC) Analysis

To further validate the expression of SERPINE1, we utilized the IF staining technique. In Huh7 cells, the group treated with HC-NPs with irradiation exhibited stronger fluorescence signals for SERPINE1 (Figure S5A), while no significant difference was observed between control group, irradiation only group, and HC-NPs only group. This suggests that HC-NPs-PDT can enhance the expression of SERPINE1 in Huh7 cells, which is consistent with previous findings.

Then, we conducted IHC analysis on subcutaneous tumors in nude mice. Consistent with the in vitro findings, HC-NPs-PDT resulted in a significant increase in SERPINE1 expression in subcutaneous tumors (Figure S5B). These combined results from both in vitro and in vivo experiments demonstrate the effective upregulation of SERPINE1 expression in HCC cells by HC-NPs-PDT.

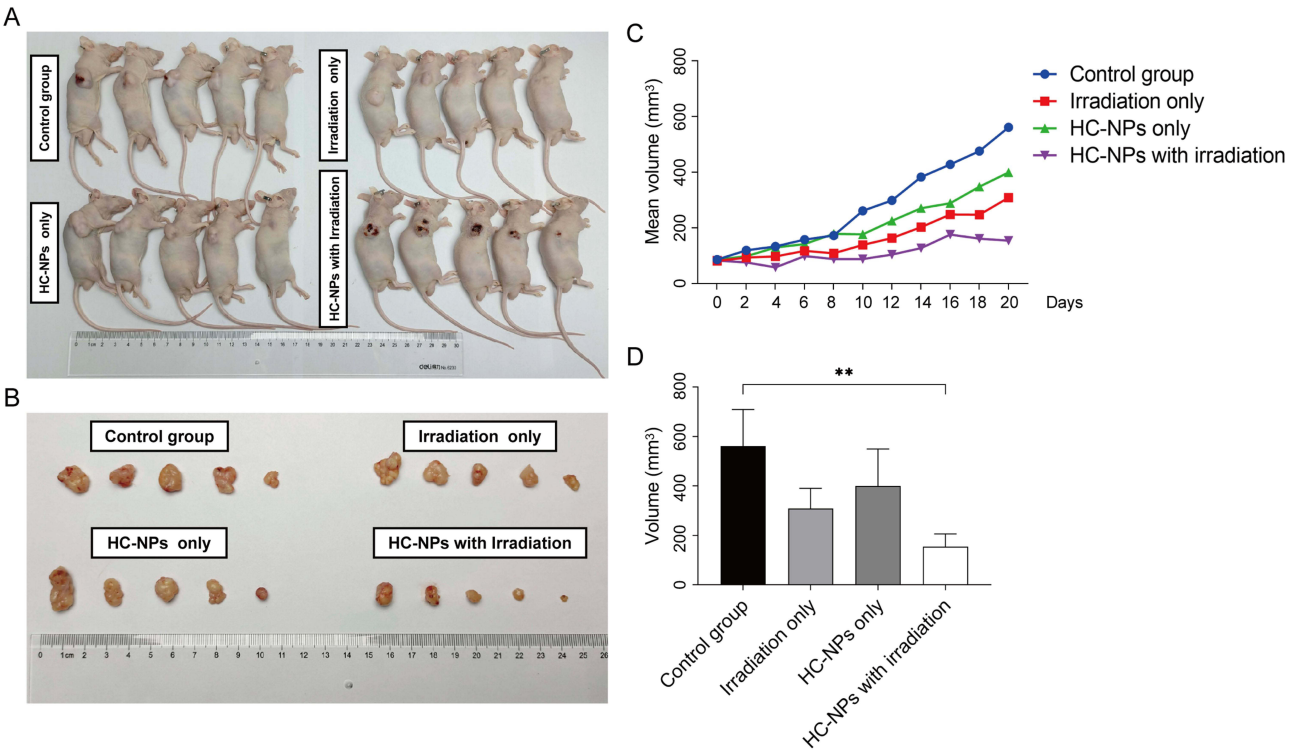

Figure 8 Statistics of subcutaneous tumors and in vivo PDT efficacy in nude mice. (**A** and **B**) represent the subcutaneous tumors in each group of nude mice at the end of treatment; (**C**) represents the change in the volume of subcutaneous tumors in each group at the end of treatment; and (**D**) represents the volume of subcutaneous tumors at the end of treatment, (**p<0.01).

Discussion

Several recent studies have suggested that PDT, previously used for treating skin diseases, may also hold potential as an anticancer treatment.[21,22] Compared to traditional anticancer therapies, PDT offers several advantages such as minimal invasiveness, low systemic toxicity, and the possibility of being combined with conventional treatments. Furthermore, it can be utilized in patients with relatively poor physical conditions. HC is considered a promising natural photosensitizer, with previous research indicating its potential effectiveness in the treatment of liver diseases.[23,24]

In this study, HC-NPs were synthesized through a nanoprecipitation encapsulation technique by combining DSPE-PEG2000 with HC in tetrahydrofuran (THF). The nano-wrapped HC demonstrated a significantly enhanced inhibitory effect on HCC cells and flow cytometry showed human HCC cells (Bel-7402 and Huh7) were induced to apoptosis, which is consistent with the findings of Arani et al, who showed that HC induces apoptosis in K562 cells through the downregulation of MYC and MDM2.[25] Additionally, other studies have shown that HC can selectively target cancer cells and induce apoptosis without harming normal cells, indicating its favorable biocompatibility.[20,26] Similarly, we also verified the significant tumor inhibition effect of HC-NPs-associated photodynamic therapy in subcutaneous tumor in nude mice, without side effects on liver function. This may be attributed to the subcellular targeting of cells by HC in combination with photodynamic therapy. David et al identified the effector targets of HC in combination with photodynamic therapy using specific fluorescent probes and concluded that the subcellular localization of HC mainly involves the endoplasmic reticulum and lysosomes, without observing a decrease in mitochondrial potential.[27] In contrast, our study found that HC-NPs-PDT caused a decrease in mitochondrial membrane potential of HCC cells as determined by JC-1 assay, which differs from the findings reported by David et al. It is hypothesized that this discrepancy may be related to differences in cell lines, tissues or tumor microenvironments.

In this study, we identified a molecular target associated with HC-NPs-PDT (SEPRINE1), which is the predominant plasminogen activator inhibitor belonging to the family of serine protease inhibitors. It can bind to urokinase-type plasminogen activator (uPA), blocking the plasmin creation by uPA. SEPRINE1 plays a crucial role in the fibrinolytic system and is involved in various biological processes such as thrombolysis, wound healing, cell migration, and tissue remodeling.[28] The current study showed that the expression level of SEPRINE1 is associated with a variety of pathological processes, including cardiovascular disease, tumor development and metastasis, and diabetes.[29–32] At present, our findings showed that HC-NPs-PDT exhibits tumor-suppressive properties, including reduced cell growth, decreased invasion and migration capabilities, and increased apoptosis. Concurrently, the mRNA and protein levels of SERPINE1 in the cells were found to be significantly upregulated over time, accompanied by a decrease in P53 levels. These results suggest that HC-NPs-PDT may enhance cell apoptosis through the upregulation of SERPINE1 expression. These results are in line with the study conducted by Inoue et al, where they demonstrated that transfecting SERPINE1 into the highly metastatic human pancreatic cancer cell line SW1990 led to the inhibition of cell invasion, in vivo tumor formation, and liver metastasis.[33] In alignment with our findings in this study, the mRNA and protein levels of SERPINE1 were significantly upregulated in Bel-7402 and Huh7 cells following HC-NPs-PDT, and the cell migration and invasion abilities were significantly inhibited. Recently, SERPINE1 up-regulation was shown to inhibit the migration of prostate cancer DU145 cells, while inhibiting SERPINE1 reduced this migration inhibition.[34] In addition, it has been reported that the natural compound berberine can inhibit the invasion and migration abilities of HCC cells by upregulating SERPINE1.[35] The biological function of SERPINE1 varies in different cancers. Some studies suggest that SERPINE1 has tumor suppressor potential, while other reports indicate that SERPINE1 tends to promote tumor development.[36,37] Wang et al found that SERPINE1 expression is low in HCC, and high expression is associated with poor prognosis, the increased expression of SERPINE1 in several other tumors corresponds to a poorer prognosis. Marquard et al[38] found that SERPINE1 is regulated by YAP and linked to tumor progression. Hong et al[39] showed that CD248 inhibits Wnt signaling and upregulates OPN and SERPINE1 in pericytes, promotes angiogenesis and lung cancer growth. In oral squamous cell carcinoma circFNDC3B drives epithelial-mesenchymal transition (EMT) or partial-EMT and lymph node metastasis by upregulating SERPINE1 and PROX1 via miR-181c-5p sequestration.[32] In our study, although the classical ROS-HIF1α-SERPINE1 resistance pathway exists for PDT,[40,41] our pharmacological molecular modeling results indicate that HC has a high affinity for SERPINE1. Therefore, we hypothesize that the direct action of

the drug distinct from the ROS pathway, may partially alter the biological effects of SERPINE1 on tumors, although the mechanism is not yet fully understood. As the liver is the main site where the coagulation and fibrinolysis systems function, the anticancer effect of SERPINE1 in HCC may be mediated by inhibiting uPA. There is increasing evidence for involvement of SERPINE1 in cell migration, tumor invasion, and metastasis. Growth of some tumors can be attenuated by SERPINE1.[37] Such as Sawai have found that activation of PPARγ by ligands decreases pancreatic cancer cell invasion through increasing PAI-1 and decreasing the uPA level.[42] And Pang et al observed that PPARγ activation decreases liver cancer cell invasion by specific PPARγ-dependent regulation of SERPINE1.[43] Therefore, the role of SERPINE1 in HCC is complex and may be mediated through inflammatory responses, changes in the tumor microenvironment, and alterations in angiogenesis. Further research is needed to elucidate this role.

The present study focused on investigating the impact of HC-NPs-PDT on HCC cells and elucidating its potential mechanism through in vitro experiments and a subcutaneous xenograft tumor model in nude mice. Although some progress has been made, there are still certain limitations that need to be addressed. Firstly, the specific molecular mechanism of HC-NPs-PDT remains unclear. Recent studies have suggested a possible association between ROS, P53/Smad, and SERPINE1,[44–46] but the details are still unclear. In the future, we plan to investigate the specific mechanisms involved in order to better understand their roles in the treatment of HCC. Additionally, it is important to consider that the effect of PDT may be limited by conditions such as low oxygen status of HCC tissues in the treatment area or excessive tumor volume. Therefore, we will explore the use of superior nanomaterials, such as auto-luminescence nanomaterials, and consider incorporating hydrogen peroxide or oxygen-containing groups into HC or other drug formulations to increase local oxygen concentration in future studies. Finally, two human HCC cell lines, Bel-7402 and Huh7, were mainly used in this study. In order to further validate the universality and clinical significance of our findings, we intend to incorporate additional types of human-derived HCC cell lines or human-derived HCC primary cells in future studies. In conclusion, our study confirms the potential of HC-NPs-PDT in antitumor therapy for HCC, offering a new perspective for the clinical treatment of this disease.

Conclusion

The main findings of this study are as follows: (1) HC-NPs-PDT significantly suppressed the cellular viability, migration, and invasive ability of HCC cells; (2) HC-NPs-PDT effectively inhibited the further growth of subcutaneous HCC tumors in BALB/C-nu nude mice; and (3) HC-NPs-PDT not only induced apoptosis of HCC cells and reduced the mitochondrial membrane potential but also modulated the biological behaviors of HCC cells by upregulating the expression of SERPINE1.

Abbreviations

PDT, Photodynamic therapy; HC, Hypericin; HCC, Hepatocellular carcinoma; HC-NPs, Hypericin nanoparticles; HC-NPs-PDT, Hypericin nanoparticles -associated photodynamic therapy; ROS, Reactive oxygen species; DSPE-PEG2000, 1.2-distearoyl-sn-glycero-3-phosphoethanolamine-N-[methoxy(polyethyleneglycol)2000].

Data Sharing Statement

The data presented in this study are available on request from the corresponding author.

Ethics Approval and Consent to Participate

The study was conducted in accordance with the *Guidance for the Care and Use of Laboratory Animals* and obtained ethical approval from the Ethics Committee of Guilin Medical University (ethical review number: GLMC-IACUC-20241055).

Acknowledgments

We sincerely thank Prof. Hongsong Chen (Institute of Liver Diseases, Peking University) for generously donating cells and the support provided by the Guilin Medical University.

Author Contributions

All authors made a significant contribution to the work reported, whether that is in the conception, study design, execution, acquisition of data, analysis and interpretation, or in all these areas; took part in drafting, revising or critically reviewing the article; gave final approval of the version to be published; have agreed on the journal to which the article has been submitted; and agree to be accountable for all aspects of the work.

Funding

This work was supported in part by the National Natural Science Foundation of China (No. 81773148), the Natural Science Foundation of Guangxi (No. 2018GXNSFDA138001), the Key Laboratory of Early Prevention and Treatment for Regional High Frequency Tumor (Guangxi Medical University), Ministry of Education; Guangxi Key Laboratory of Early Prevention and Treatment for Regional High Frequency Tumor (no. GKE-KF202208), the Project Program of Guangxi Key Laboratory of Drug Discovery and Optimization (no. GKLPMDDO-2022-C04, GKLPMDDO-2022-C05) and the Program of Guangxi Zhuang Autonomous Region health and Family Planning Commission (no. Z-C20220826).

Disclosure

The authors report no conflicts of interest in this work.

References

1. Bray F, Laversanne M, Sung HYA, et al. Global cancer statistics 2022: GLOBOCAN estimates of incidence and mortality worldwide for 36 cancers in 185 countries. *Ca-Cancer J Clin*. 2024;74(3):229–263. doi:10.3322/caac.21834
2. Forner A, Reig M, Bruix J. Hepatocellular carcinoma. *Lancet*. 2018;391(10127):1301–1314. doi:10.1016/S0140-6736(18)30010-2
3. Raza A, Sood GK. Hepatocellular carcinoma review: current treatment, and evidence-based medicine. *World J Gastroenterol*. 2014;20 (15):4115–4127. doi:10.3748/wjg.v20.i15.4115
4. Rougier P, Mitry E, Barbare JC, Taieb J. Hepatocellular carcinoma (HCC): an update. *Semin Oncol*. 2007;34(2 Suppl 1):S12–20. doi:10.1053/j.seminoncol.2007.01.007
5. Brown ZJ, Tsilimigras DI, Ruff SM, et al. Management of hepatocellular carcinoma: a review. *JAMA Surg*. 2023;158(4):410–420. doi:10.1001/jamasurg.2022.7989
6. Chang Lee R, Tebbutt N. Systemic treatment of advanced hepatocellular cancer: new hope on the horizon. *Expert Rev Anti Therap*. 2019;19 (4):343–353. doi:10.1080/14737140.2019.1585245
7. Xing R, Gao J, Cui Q, Wang Q. Strategies to improve the antitumor effect of immunotherapy for hepatocellular carcinoma. *Front Immunol*. 2021;12:783236. doi:10.3389/fimmu.2021.783236
8. Ladd AD, Duarte S, Sahin I, Zarrinpar A. Mechanisms of drug resistance in HCC. *Hepatology*. 2024;79(4):926–940. doi:10.1097/HEP.0000000000000237
9. Jiang L, Liu L, Lv F, Wang S, Ren X. Integration of self-luminescence and oxygen self-supply: a potential photodynamic therapy strategy for deep tumor treatment. *Chempluschem*. 2020;85(3):510–518. doi:10.1002/cplu.202000083
10. Zhong Y, Bejjanki NK, Miao X, et al. Synthesis and photothermal effects of intracellular aggregating nanodrugs targeting nasopharyngeal carcinoma. *Front Bioeng Biotechnol*. 2021;9:730925. doi:10.3389/fbioe.2021.730925
11. Hsu CW, Cheng NC, Liao MY, Cheng TY, Chiu YC. Development of folic acid-conjugated and methylene blue-adsorbed Au@TNA nanoparticles for enhanced photodynamic therapy of bladder cancer cells. *Nanomaterials*. 2020;10(7):1351. doi:10.3390/nano10071351
12. Zhu X, Yu Z, Feng L, et al. Chitosan-based nanoparticle co-delivery of docetaxel and curcumin ameliorates anti-tumor chemoimmunotherapy in lung cancer. *Carbohydr Polym*. 2021;268:118237. doi:10.1016/j.carbpol.2021.118237
13. Wu JJ, Zhang J, Xia CY, et al. Hypericin: a natural anthraquinone as promising therapeutic agent. *Phytomedicine*. 2023;111:154654. doi:10.1016/j.phymed.2023.154654
14. Peng Z, Lu J, Liu K, et al. Hypericin as a promising natural bioactive naphthodianthrone: a review of its pharmacology, pharmacokinetics, toxicity, and safety. *Phytotherap Res*. 2023;37(12):5639–5656. doi:10.1002/ptr.8011
15. Choudhary N, Collignon TE, Tewari D, Bishayee A. Hypericin and its anticancer effects: from mechanism of action to potential therapeutic application. *Phytomedicine*. 2022;105:154356. doi:10.1016/j.phymed.2022.154356
16. Woźniak M, Nowak-Perlak M. Hypericin-based photodynamic therapy displays higher selectivity and phototoxicity towards melanoma and squamous cell cancer compared to normal keratinocytes in vitro. *Int J mol Sci*. 2023;24(23):16897. doi:10.3390/ijms242316897
17. Guo NK, She H, Tan L, et al. Nano parthenolide improves intestinal barrier function of sepsis by inhibiting apoptosis and ROS via 5-HTR2A. *Int J Nanomedicine*. 2023;18:693–709. doi:10.2147/IJN.S394544
18. Liang T, Jing P, He J. Nano techniques: an updated review focused on anthocyanin stability. *Crit Rev Food Sci Nutri*. 2023;1–24.
19. Zhang Y, Wu Y, Du H, et al. Nano-drug delivery systems in oral cancer therapy: recent developments and prospective. *Pharmaceutics*. 2023;16 (1):7. doi:10.3390/pharmaceutics16010007
20. Ke Z, Xie A, Chen J, et al. Naturally available hypericin undergoes electron transfer for type I photodynamic and photothermal synergistic therapy. *Biomater Sci*. 2020;8(9):2481–2487. doi:10.1039/D0BM00021C
21. de Oliveira AB, Ferrisse TM, Fontana CR, Basso FG, Brighenti FL. Photodynamic therapy for treating infected skin wounds: a systematic review and meta-analysis from randomized clinical trials. *Photodiagnosis Photodyn Ther*. 2022;40:103118. doi:10.1016/j.pdpdt.2022.103118

22. Carigga Gutierrez NM, Pujol-Solé N, Arifi Q, Coll JL, le Clainche T, Broekgaarden M. Increasing cancer permeability by photodynamic priming: from microenvironment to mechanotransduction signaling. *Cancer Metastasis Rev*. 2022;41(4):899–934. doi:10.1007/s10555-022-10064-0
23. Liang C, Li Y, Bai M, et al. Hypericin attenuates nonalcoholic fatty liver disease and abnormal lipid metabolism via the PKA-mediated AMPK signaling pathway in vitro and in vivo. *Pharmacol Res*. 2020;153:104657. doi:10.1016/j.phrs.2020.104657
24. Sun Y, Liang C, Zheng L, et al. Anti-fatigue effect of hypericin in a chronic forced exercise mouse model. *J Ethnopharmacol*. 2022;284:114767. doi:10.1016/j.jep.2021.114767
25. Arani HZ, Olya M, Mirahmadi AS, et al. Hypericin induces apoptosis in K562 cells via downregulation of Myc and Mdm2. *J Cancer Res Therape*. 2021;17(1):242–247. doi:10.4103/jcrt.JCRT_826_19
26. Naderi M, Rahmani Cherati M, Mohammadian A, et al. Hypericin induces apoptosis in AGS cell line with no significant effect on normal cells. *Iranian J Pharmace Res*. 2020;19(3):349–357. doi:10.22037/ijpr.2019.14904.12735
27. Kessel D. Exploring Modes of Photokilling by Hypericin. *Photochem Photobiol*. 2020;96(5):1101–1104. doi:10.1111/php.13275
28. Morrow GB, Mutch NJ. Past, present, and future perspectives of plasminogen activator inhibitor 1 (PAI-1). *Semin Thromb Hemostasi*. 2023;49 (3):305–313. doi:10.1055/s-0042-1758791
29. Baumeier C, Escher F, Aleshcheva G, Pietsch H, Schultheiss HP. Plasminogen activator inhibitor-1 reduces cardiac fibrosis and promotes M2 macrophage polarization in inflammatory cardiomyopathy. *Basic Res Cardiol*. 2021;116(1):1. doi:10.1007/s00395-020-00840-w
30. Altalhi R, Pechlivani N, Ajjan RA. PAI-1 in diabetes: pathophysiology and role as a therapeutic target. *Int J mol Sci*. 2021;22(6):3170. doi:10.3390/ijms22063170
31. Chen S, Li Y, Zhu Y, et al. SERPINE1 overexpression promotes malignant progression and poor prognosis of gastric cancer. *J Oncol*. 2022;2022:2647825.
32. Li X, Wang C, Zhang H, et al. circFNDC3B accelerates vasculature formation and metastasis in oral squamous cell carcinoma. *Cancer Res*. 2023;83(9):1459–1475. doi:10.1158/0008-5472.CAN-22-2585
33. Inoue M, Sawada T, Uchima Y, et al. Plasminogen activator inhibitor-1 (PAI-1) gene transfection inhibits the liver metastasis of pancreatic cancer by preventing angiogenesis. *Oncol Rep*. 2005;14(6):1445–1451.
34. Mao Y, Li W, Hua B, et al. Silencing of ELK3 induces S-M phase arrest and apoptosis and upregulates SERPINE1 expression reducing migration in prostate cancer cells. *BioMed Res Inter*. 2020;2020:2406159. doi:10.1155/2020/2406159
35. Wang X, Wang N, Li H, et al. Up-regulation of PAI-1 and down-regulation of upa are involved in suppression of invasiveness and motility of hepatocellular carcinoma cells by a natural compound berberine. *Int J mol Sci*. 2016;17(4):577. doi:10.3390/ijms17040577
36. Kubala MH, DeClerck YA. The plasminogen activator inhibitor-1 paradox in cancer: a mechanistic understanding. *Cancer Metastasis Rev*. 2019;38 (3):483–492. doi:10.1007/s10555-019-09806-4
37. Wang B, Gu B, Zhang T, et al. Good or bad: paradox of plasminogen activator inhibitor 1 (PAI-1) in digestive system tumors. *Cancer Lett*. 2023;559:216117. doi:10.1016/j.canlet.2023.216117
38. Marquard S, Thomann S, Weiler SME, et al. Yes-associated protein (YAP) induces a secretome phenotype and transcriptionally regulates plasminogen activator Inhibitor-1 (PAI-1) expression in hepatocarcinogenesis. *Cell Commun Signal*. 2020;18(1):166. doi:10.1186/s12964-020-00634-6
39. Hong CL, Yu IS, Pai CH, et al. CD248 regulates Wnt signaling in pericytes to promote angiogenesis and tumor growth in lung cancer. *Cancer Res*. 2022;82(20):3734–3750. doi:10.1158/0008-5472.CAN-22-1695
40. Broekgaarden M, Weijer R, van Gulik TM, Hamblin MR, Heger M. Tumor cell survival pathways activated by photodynamic therapy: a molecular basis for pharmacological inhibition strategies. *Cancer Metastasis Rev*. 2015;34(4):643–690. doi:10.1007/s10555-015-9588-7
41. Weijer R, Broekgaarden M, van Golen RF, et al. Low-power photodynamic therapy induces survival signaling in perihilar cholangiocarcinoma cells. *BMC Cancer*. 2015;15(1):1014. doi:10.1186/s12885-015-1994-2
42. Sawai H, Liu J, Reber HA, Hines OJ, Eibl G. Eibl G: activation of peroxisome proliferator-activated receptor-gamma decreases pancreatic cancer cell invasion through modulation of the plasminogen activator system. *Molecular Cancer Res*. 2006;4(3):159–167. doi:10.1158/1541-7786.MCR-05-0257
43. Pang X, Wei Y, Zhang Y, Zhang M, Lu Y, Shen P. Peroxisome proliferator-activated receptor-γ activation inhibits hepatocellular carcinoma cell invasion by upregulating plasminogen activator inhibitor-1. *Cancer Sci*. 2013;104(6):672–680. doi:10.1111/cas.12143
44. Cao J, Liu X, Yang Y, et al. Decylubiquinone suppresses breast cancer growth and metastasis by inhibiting angiogenesis via the ROS/p53/ BAI1 signaling pathway. *Angiogenesis*. 2020;23(3):325–338. doi:10.1007/s10456-020-09707-z
45. Wang JN, Yang Q, Yang C, et al. Smad3 promotes AKI sensitivity in diabetic mice via interaction with p53 and induction of NOX4-dependent ROS production. *Redox Biol*. 2020;32:101479. doi:10.1016/j.redox.2020.101479
46. Zhang L, Cao Y, Guo X, et al. Hypoxia-induced ROS aggravate tumor progression through HIF-1α-SERPINE1 signaling in glioblastoma. *J Zhejiang Univ Sci B*. 2023;24(1):32–49. doi:10.1631/jzus.B2200269